Two-Frequency Separated Oscillating Fields Technique for Atomic and Molecular Beam Spectroscopy

R. MICHAEL GARVEY, HELMUT W. HELLWIG, SENIOR MEMBER, IEEE, STEPHEN JARVIS, JR., AND DAVID J. WINELAND

INTRODUCTION

THE RAMSEY TECHNIQUE [1] of separated oscillating fields for atomic beam spectroscopy is widely used in atomic frequency standards, specifically in the cesium beam standard which forms the present basis for the definition of frequency and time interval. The technique offers the advantages of narrow linewidth, relative freedom from first-order Doppler effects, relaxation of certain constraints on field homogeneity in the drift region, and relative ease of implementation.

A difference δ in the phase of the interrogating RF signals as experienced by the atomic beam in the two Ramsey interaction regions leads to a displacement of the maximum transition probability from the true atomic resonance frequency by $\sim \delta/\langle T\rangle$ where $\langle T\rangle$ represents the average flight time between the interaction regions. Care in fabrication and assembly of atomic beam apparatus may reduce but cannot ultimately eliminate this source of error. Beam reversal, a procedure which is only practical for laboratory devices, yields information on the value of δ, but the accuracy of this technique is limited by a similar effect, that of "distributed" phase error, which occurs as a result of a phase change across the transverse dimension of the interaction region. This latter effect is much less tractable in analytical treatment [2]. These two effects are presently the most serious source of uncertainty in the evaluation of primary frequency standards. In NBS 6, the U.S. primary cesium frequency standard, phase-shift effects limit the accuracy to $\sim 10^{-13}$. The long-term stability ($\sim 10^{-14}$) may also be limited by phase-shift effects. In commercial cesium standards phase-shift effects may be major contributors to inaccuracy and long-term drift.

We are attacking the phase-shift problem by relaxing the constraint $\delta = 0$ and allowing the relative phase of the two interaction regions to advance (or recede) at a constant rate [3]. This will be implemented by driving the two spatially separated cavities each with a different frequency near the cesium atomic resonance. Fig. 1 depicts such an interrogation scheme. The transition probability of an atom traversing such a configuration depends upon the relative RF phases encountered by the atom in the two field regions. In the two-frequency configuration, the relative phase of the two RF regions is a time varying parameter due to the offset (in frequency) of the two RF signals. The phase difference, as observed by the atoms, is thus also time varying producing a time varying transition probability whose magnitude is unaffected by the initial relative phase of the two RF signals.

The accuracy with which the atomic resonance may be measured thus does not depend upon the ability of the experimenter to set and maintain a static value of phase between the two RF regions (as in the single-frequency Ramsey configuration).

Detection of the atomic line center does require some special techniques, however. We consider below the theory of two-frequency atomic beam interrogation and the specific requirements for accurately measuring the atomic line center.

THEORY

The transition probability for an atom experiencing two separated RF fields of frequency ω_1 and ω_2 near the atomic resonant frequency ω_0, and separated from each other in frequency by 2Ω ($2\Omega \equiv \omega_2 - \omega_1$; Ω may be negative), may be developed directly without approximation from the time-dependent Schrödinger equation as in Ramsey's treatment [1]. For an atom arriving at the detector at time t (see Fig. 1) the transition probability is

$$P(t) = A_0 + B_0 \cos 2\Omega t - C_0 \sin 2\Omega t \tag{1}$$

where

$$A_0 = \sum_{r=11}^{15} k_r \cos m_r T \tag{2}$$

$$B_0 = \sum_{r=1}^{10} k_r \cos (m_r T + \delta_0) \tag{3}$$

$$C_0 = \sum_{r=1}^{10} k_r \sin (m_r T + \delta_0) \tag{4}$$

where coefficients k and m are given in Table I; T is the time of flight between interaction regions, and δ_0 is the phase lead of the signal in cavity 2 with respect to the signal in cavity 1 at $t = 0$. It is convenient to define frequencies with respect to

Manuscript received July 17, 1978; revised July 27, 1978.

The authors are with the Time and Frequency Division, National Bureau of Standards, Boulder, CO 80303.

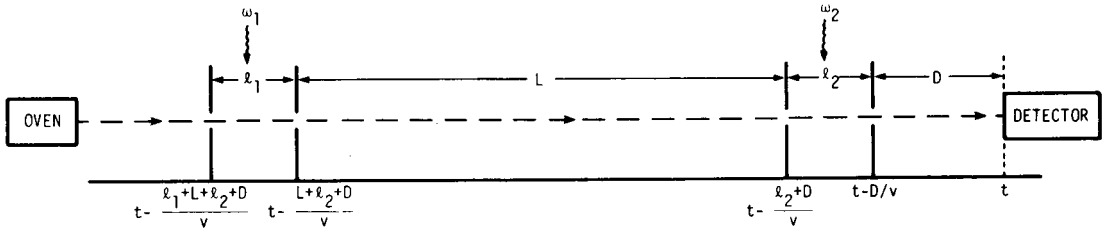

Fig. 1. Timing chart for atoms arriving at detector at time t.

TABLE I

r	k_r	m_r
1	$-S_1S_2(C_1-1)(C_2-1)$	$\gamma + (\eta_1+\eta_2)$
2	$-S_1S_2(C_1+1)(C_2+1)$	$\gamma - (\eta_1+\eta_2)$
3	$-S_1S_2(C_1-1)(C_2+1)$	$\gamma + (\eta_1-\eta_2)$
4	$-S_1S_2(C_1+1)(C_2-1)$	$\gamma - (\eta_1-\eta_2)$
5	$2S_1S_2(C_1-1)C_2$	$\gamma + \eta_1$
6	$2S_1S_2(C_1+1)C_2$	$\gamma - \eta_1$
7	$2S_1S_2C_1(C_2-1)$	$\gamma + \eta_2$
8	$2S_1S_2C_1(C_2+1)$	$\gamma - \eta_2$
9	$-2S_1S_2C_1C_2$	γ
10	$-2S_1S_2C_1C_2$	γ
11	$2S_1^2(C_2^2+1) + 2S_2^2(C_1^2+1)$	0
12	$S_1^2(C_2^2-1) + S_2^2(C_1^2-1)$	$\eta_1 + \eta_2$
13	$S_1^2(C_2^2-1) + S_2^2(C_1^2-1)$	$\eta_1 - \eta_2$
14	$-2S_1^2(C_2^2+1) - 2S_2^2(C_1^2-1)$	η_1
15	$-2S_1^2(C_2^2-1) - 2S_2^2(C_1^2+1)$	η_2

$S_j \equiv -\frac{2b_j}{a_j}$ $\quad a_j = \sqrt{\lambda_j^2+4b_j^2}$ $\quad \lambda_j \equiv \omega_j-\omega_0$

$C_j \equiv -\frac{\lambda_j}{a_j}$ $\quad \bar{\lambda} \equiv \frac{1}{2}(\lambda_1+\lambda_2)$ $\quad \gamma \equiv \lambda_2\mu-\lambda_1(\mu+1)$

$\eta_j \equiv a_j\frac{l_j}{L}$ $\quad \gamma = (2\mu+1)\Omega-\bar{\lambda}$ $\quad \mu = \frac{D+l_2}{L}$

the atomic resonance: $\lambda_j = \omega_j - \omega_0$. (Note that this differs in sign from [1].) We also construct the average frequency $\bar{\lambda} = \frac{1}{2}(\lambda_1 + \lambda_2)$. These defining relationships are included in Table I.

The signal of interest is the envelope of $P(t)$ which may be generated analytically by the appropriate velocity and trajectory averages

$$\mathscr{E}^2 = \langle B_0\rangle^2 + \langle C_0\rangle^2. \tag{5}$$

For the near resonance condition $\lambda_j \ll 2b_j$ (see Table I), (3) and (4) may be simplified to yield

$$B_0 = X \sin(\gamma T + \delta_0) + Y \cos(\gamma T + \delta_0) \tag{6}$$

$$C_0 = Y \sin(\gamma T + \delta_0) - X \cos(\gamma T + \delta_0) \tag{7}$$

$$X = \frac{4\bar{\lambda}}{b} \sin(\eta T)(\cos(\eta T) - 1) \tag{8}$$

$$Y = (\cos(\eta T) - 1) \cdot \left[\frac{\Omega^2 - \bar{\lambda}^2}{b^2}(\cos(\eta T) - 1) - 4(\cos(\eta T) + 1)\right] \tag{9}$$

where $\bar{\lambda}$ is the average offset frequency

$$\bar{\lambda} = \frac{\omega_1 + \omega_2}{2} - \omega_0 = \tfrac{1}{2}(\lambda_1 + \lambda_2)$$

and 2Ω is the difference frequency. γ is a frequency $\gamma = (2\mu + 1)\Omega - \bar{\lambda}$; $\mu = (l_2 + D)/L$ which in the limits of $\Omega = 0$ (conventional single-frequency two-cavity Ramsey configuration) becomes $\bar{\lambda}$, the offset of the interrogating signal from resonance. η is a factor relating to interrogating power level and is defined in Table I. Note that γ is related to system geometry through the parameter μ.

Neglecting, for the moment, the possible effects of different atomic trajectories (causing a spatial dependence of the cavity phase shift), we may form the velocity averaged functions $\langle B_0\rangle^2$ and $\langle C_0\rangle^2$ to generate an expression for the envelope

$$\mathscr{E}^2 = \int_0^\infty \int_0^\infty \rho_A\rho_B\{B_0(T_A)B_0(T_B) + C_0(T_A)C_0(T_B)\}\, dT_A\, dT_B \tag{10}$$

where ρ_A and ρ_B denote the distribution of periods T_A and T_B appropriate for the atomic beam velocity distribution. Algebraic manipulation of (6), (7), and (10) reveal that, at this level of approximation, $\mathscr{E}$ is independent of δ_0, the cavity phase shift. This is a result of the absence of trajectory averaging (see below). Equation (10) may be easily evaluated for effusive beam velocity distributions using the functions $I(x)$ and $K(x)$ of Kruse and Ramsey [4]. The largest term in this expression is (recall the assumption $\lambda \ll b$)

$$\begin{aligned}\mathscr{E}_1^2(\gamma) = \{&I(\gamma L/\alpha) - I(\gamma L/\alpha + 4bl/\alpha) \\ &- I(\gamma L/\alpha - 4bl/\alpha)\}^2 \\ &+ \{K(\gamma L/\alpha) - K(\gamma L/\alpha + 4bl/\alpha) \\ &- K(\gamma L/\alpha - 4bl/\alpha)\}^2\end{aligned} \tag{11}$$

where α is the characteristic velocity of the distribution. The two squared terms in (11) are the normal Ramsey spectral shapes for zero and $\pi/2$ phase difference between the two interaction regions (see [1, eqs. (V.46) and (V.47)]). Optimum power occurs for $4bl/\alpha = 1.2\pi$ as in the single-frequency separated oscillatory fields technique. Fig. 2 shows the two Ramsey curves and the envelope generated by scanning $\bar{\lambda}$.

Consideration of (10) reveals that $\mathscr{E}_1^2$ is symmetric about

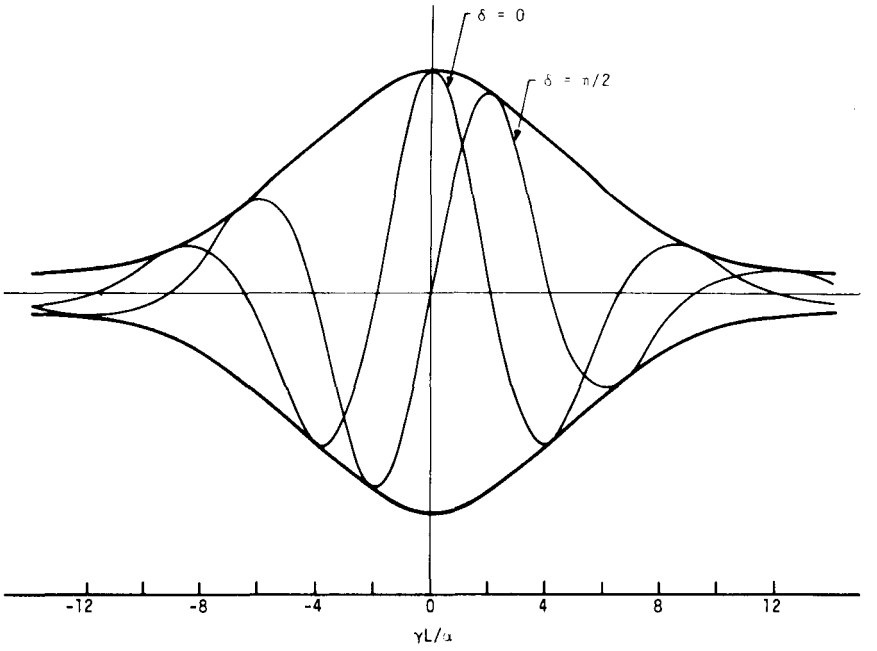

Fig. 2. Ramsey spectral shapes for zero and $\pi/2$ phase difference and the limiting envelope.

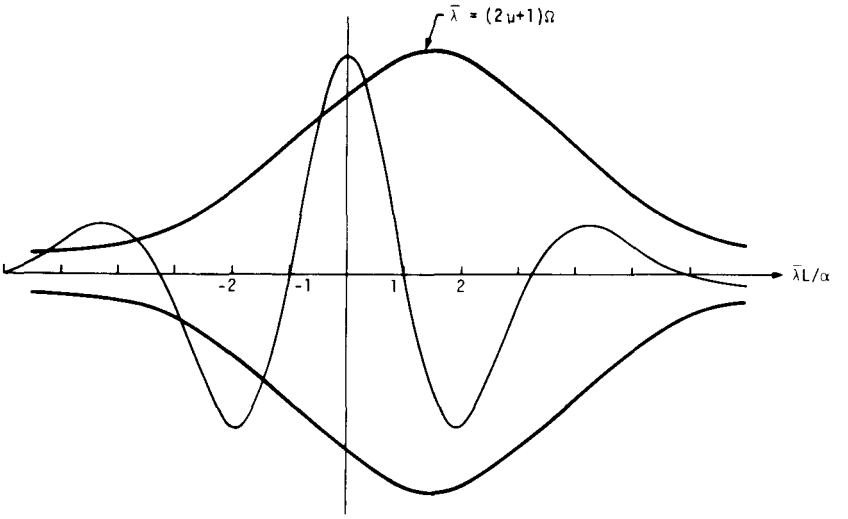

Fig. 3. Envelope intensity versus average frequency.

$\gamma = 0$ [$\gamma = (2\mu + 1)\Omega - \bar{\lambda}$]. Assuming, for the moment, $\mu = 0$ (which is equivalent to instantaneous detection at the second cavity), maximum signal occurs for no offset in cavity 1 ($\lambda_1 = 0$, $\lambda_2 = 2\Omega$). This maximum may be understood from the following classical argument. Atoms passing through cavity 1 are prepared, in a sense, by exposure to radiation in that cavity. If cavity 1 is driven at the atoms' resonant frequency $\omega_0 = (\bar{W}_q - \bar{W}_p)/\hbar$ the individual precessions of all atoms remain in phase with the radiation in cavity 1 as these atoms drift through the C-field region. Atoms entering cavity 2 at a particular instant are all in phase with cavity 1 (regardless of when they left cavity 1); as a consequence, the relative phase of the two fields as seen by the atoms is the same for all atoms in cavity 2 at any given instant. The phase difference as observed by the atoms entering cavity 2 at a given instant is thus not a function of the atoms' velocities (nor times of flight) but is a function of time through the time varying phase between cavities 1 and 2: $\delta(t) = \delta_0 + 2\Omega t$. Any configuration in which cavity 1 is off resonance produces a phase shift (as seen by the atoms) which is velocity dependent and must thereby result in reduced signal at the detector.

Returning to the case $\mu \neq 0$, Fig. 3 shows the expected envelope generated from an effusive beam (see (20)) experiment where the average frequency $\bar{\lambda}$ is swept (since λ_1, λ_2, and γ are additively related to $\bar{\lambda}$, they are also swept) and 2Ω, the cavity difference frequency, is held constant at $2\Omega = 4\alpha/L$. (This choice for 2Ω is discussed below.) The parameter μ has been arbitrarily chosen to be 0.25. Note that the envelope peak occurs for $\bar{\lambda} = (2\mu + 1)\Omega$ (equivalently

$\gamma = 0, \lambda_1 = 2\mu\Omega, \lambda_2 = 2\Omega(\mu + 1)$). Also shown in Fig. 3 is the normal single-frequency Ramsey spectrum which would be produced in the same experimental configuration for $\Omega = 0$ (assuming cavity phase shift is zero). Examination of higher order terms in (5)–(9) reveal a small envelope antisymmetry (about $\gamma = 0$) of order Ω/b. This is not shown in Fig. 3. The curve described above is not a suitable reference for an atomic frequency standard due to the imprecision of the quantity μ.

A more comprehensive examination of (1)–(4) is necessary to fully investigate other envelope symmetries and to consider the effects of beam trajectory averaging. As in (5) we form

$$\mathscr{E}^2 = \langle B_0 \rangle^2 + \langle C_0 \rangle^2 \tag{12}$$

where $\langle\ \rangle$ denotes an average over velocity and over trajectory. More explicitly

$$\mathscr{E}^2(\bar{\lambda}, \Omega) = \iint d\boldsymbol{P}_C\, d\boldsymbol{P}_D \iint dT_A\, dT_B \rho_{AC} \rho_{BD} \cdot \sum_{r=1}^{10} \sum_{s=1}^{10} k_{rC} k_{sD} \cos\,(m_{rC} T_A - m_{sD} T_B + \delta_C - \delta_D) \tag{13}$$

where $\boldsymbol{P}_C, \boldsymbol{P}_D$ are a pair of parameter vectors describing pairs of detectable trajectories and T_A, T_B cover all pairs of velocities, the functional notation being $\rho(T_A, \boldsymbol{P}_C) = \rho_{AC}$, $k_r(\boldsymbol{P}_C) = k_{rC}$, $\delta(\boldsymbol{P}_C) = \delta_C$, etc. We assume $\boldsymbol{P} = \boldsymbol{P}_1 \otimes \boldsymbol{P}_2$ describes the intercavity trajectory using coordinates $\boldsymbol{P}_j$ in cavity j. Note that the phase difference of different trajectories C, D is equivalent to the distributed phase difference for the two cavities 1, 2

$$\begin{aligned} \delta_C - \delta_D &= (\phi(\boldsymbol{P}_{2C}) - \phi(\boldsymbol{P}_{1C})) - (\phi(\boldsymbol{P}_{2D}) - \phi(\boldsymbol{P}_{1D})) \\ &= (\phi(\boldsymbol{P}_{2C}) - \phi(\boldsymbol{P}_{2D})) - (\phi(\boldsymbol{P}_{1C}) - \phi(\boldsymbol{P}_{1D})) \\ &\equiv \Delta_{CD}. \end{aligned} \tag{14}$$

Assuming $\Delta_{CD} \ll 1$, (13) becomes

$$\mathscr{E}^2(\bar{\lambda}, \Omega) = \iint d\boldsymbol{P}_C\, d\boldsymbol{P}_D \iint dT_A\, dT_B \rho_{AC} \rho_{BD} \sum_{r,s=1}^{10} k_{rC} k_{sD} \{\cos\,(m_{rC} T_A - m_{sD} T_B) - \Delta_{CD} \sin\,(m_{rC} T_A - m_{sD} T_B)\}. \tag{15}$$

One concludes from (15) that $\mathscr{E}$ is independent of δ_0, the initial cavity-to-cavity phase shift, but $\mathscr{E}$ does depend upon the distributed cavity phase shift.

Note, in Table I, that the operation $\chi(\bar{\lambda} \to -\bar{\lambda}; \Omega \to -\Omega)$ preserves λ_j^2, a_j, and S_j while changing the sign of λ_j, γ, and C_j (assuming b_j independent of λ_j to first order). As for k and m

$$k_{2r-1} \overset{\chi}{\leftrightarrow} k_{2r} \tag{16}$$

$$m_{2r-1} \overset{\chi}{\leftrightarrow} -m_{2r} \tag{17}$$

and the sum

$$\sum_{r,s=1}^{10} k_{rC} k_{sD} \cos\,(m_{rC} T_A - m_{sD} T_B) \tag{18}$$

is unchanged, while

$$\sum_{r,s=1}^{10} k_{rC} k_{sD} (-\Delta_{CD}) \sin\,(m_{rC} T_A - m_{sD} T_B) \tag{19}$$

changes sign. Thus the envelope $\mathscr{E}$ of (15) contains a term symmetric under χ (18) and a term antisymmetric under χ (19). The latter term, which represents the effects of distributed cavity phase shift, is generally small and under certain conditions described below can be made to vanish.

As demonstrated above, the cavity-to-cavity phase shift error can be eliminated by the two-frequency separated oscillating fields technique. Potentially, the distributed cavity phase shift error may also be eliminated through the use of atomic beams which are isotropic with respect to velocity distribution shape. In other words, if the trajectories (of any detected atoms) exhibit the same velocity distribution shape, though the amplitudes may vary, the bias of Δ_{CD} vanishes (i.e., $\rho(T, \boldsymbol{P}) = \rho(T)\rho(\boldsymbol{P})$). It should be noted that in the single-frequency separated fields configuration elimination of the errors of cavity phase shift is not possible via a beam with isotropic velocity distribution. Even without isotropic velocity distributions, the two-frequency technique reduces the distributed cavity phase error from one depending directly on spatial velocity distributions to one depending upon differences in velocity distribution.

Neglecting, for the moment, the effects of distributed cavity phase, we may generate the expected envelope as a function of $\bar{\lambda}$ for the two signs of Ω (Fig. 4). As in Fig. 3, we choose $2\Omega = 4\alpha/L$ and arbitrarily set $\mu = 0.25$. The envelope antisymmetry, mentioned above, is highly exaggerated for clarity. In most experiments, the antisymmetric term would be quite small (of the order $\Omega/b \simeq 10^{-2}$). Sign reversal of Ω produces a mirror imaged curve (about $\bar{\lambda} = 0$). A simultaneous reversal of the sign of $\bar{\lambda}$ and Ω produces χ, a useful and symmetric modulation.

Discussion

As shown above, the effect of distributed cavity phase shift may be removed to the extent that beam trajectory is not velocity selective. Atomic beam frequency standards universally employ magnetic deflection to achieve state selection, a process which has many aspects detrimental to the formation of isotropic beams. Optical state selection [5] and detection may be an attractive solution to this problem.

Another benefit is derived from the two-frequency interrogation technique. The useful signal at the detector occurs at 2Ω and arises from atoms undergoing transition in both cavities. Baseline pulling by the broad Rabi pedestals which are present in single-frequency separated oscillatory fields configurations is much less of a consideration. Although other effects (Majorana transitions, quantum state mixing, etc.) must be considered, it may be possible to significantly reduce the C-field magnitude. This would result in decreased sensitivity of the $M_F = 0$ transition to magnetic-field fluctuations (since its sensitivity is proportional to H^2).

The Ramsey envelope exhibits symmetry for the operation χ: $(\bar{\lambda} \to -\bar{\lambda};\ \Omega \to -\Omega)$ as shown above. Using the operation χ as a modulation allows one to find the atomic

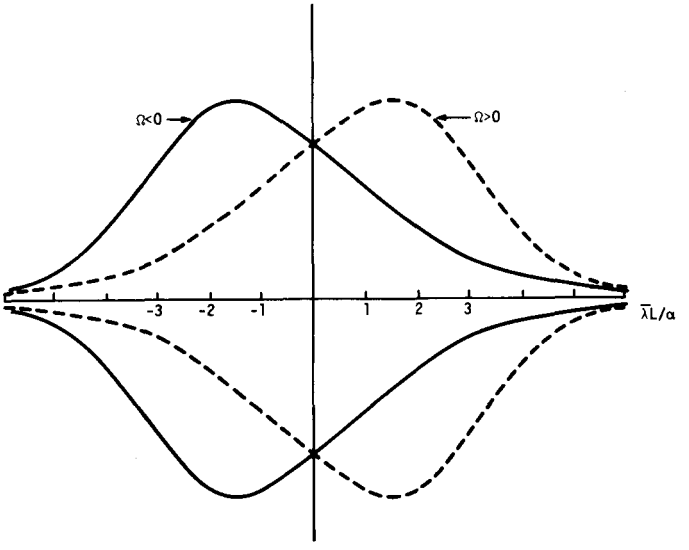

Fig. 4. Envelope intensity including antisymmetry (exaggerated) for both signs of Ω.

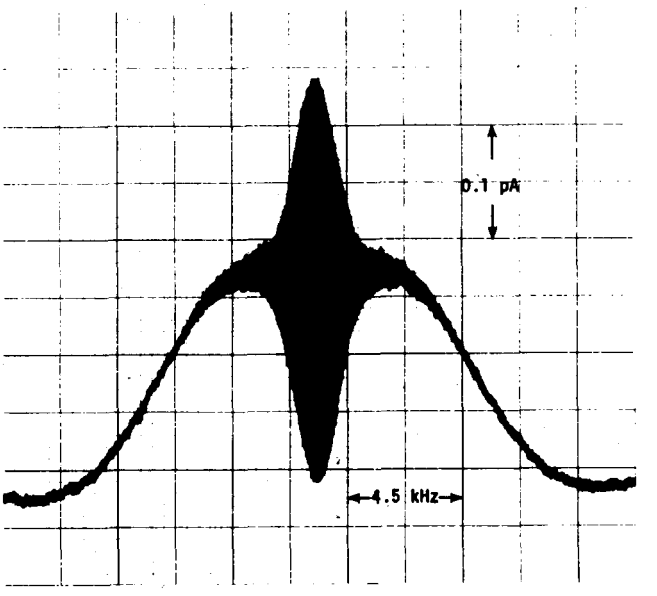

Fig. 5. Experimentally generated envelope.

resonance center. To show that this is true, consider the example of an experimental configuration. We desire to attain the following (assume $\Omega > 0$):

$$\lambda_2 = 0$$

and

$$\lambda_1 = -2\Omega$$

$$\bar{\lambda} = -\Omega.$$

λ_1 is generated with reference to λ_2. The sign of $\bar{\lambda}$ and Ω may both be changed by referencing λ_1 above λ_2 by 2Ω. The envelope amplitude is unchanged by such an operation. On the other hand, if λ_2 is in error, i.e., is not centered on the atomic resonance, referencing λ_1 above and below λ_2 by 2Ω does not produce χ, the envelope is not constant and an error signal may be generated to correct λ_2.

The calculations above and the envelope of Fig. 2 are characteristic of effusive beam velocity distributions

$$\rho \simeq (v/\alpha)^3 e^{-v^2/\alpha^2}. \tag{20}$$

The envelope shape would, of course, vary for different distributions; more narrow for broad velocity distributions and conversely. In light of the difficulty of producing beams with isotropic velocity distributions, the effusive distribution is probably the most applicable.

As shown in Fig. 2 the envelope has maximum slope at $\gamma L/\alpha \simeq 4$. For $\lambda_1 = -2\Omega$, $\lambda_2 = 0$ we may solve for a reasonable value of 2Ω

$$2\Omega \simeq 4\alpha/L$$

which is approximately equal to the normal Ramsey linewidth.

Due to the reduced signal slope, short-term stability of an atomic frequency standard employing the two-frequency technique will be somewhat worse than in the single-frequency configuration under similar experimental conditions (beam current, L, etc.). From Fig. 2, which depicts signals from an effusive velocity distribution, we may estimate the degradation to be approximately a factor of two to three. Elimination of the errors associated with cavity phase shift allows the use of broader (and thus more intense) beams, thereby permitting some recovery of this lost performance.

It is of some interest to extrapolate the performance of the primary standard NBS 6 to include the two-frequency separated oscillating fields technique. Removal of the cavity phase shift (and its uncertainty) [6] and elimination of baseline pulling by adjacent Rabi features reduces the uncertainties in accuracy to the level of $\simeq 10^{-14}$. Short-term performance could be expected to deteriorate from its present level of $\sigma_y = 7 \times 10^{-13}\tau^{-1/2}$ to approximately $\sigma_y = 2 \times 10^{-12}\tau^{-1/2}$.

An experimental program is currently under way at NBS to investigate the potential of the two-frequency separated oscillatory fields technique. A commercial cesium beam tube has been modified to operate with two separate frequencies. Conventional magnetic state selection is being retained for the initial stages of this experiment. Fig. 5 shows a generated envelope for the $M_F = 0$ transition. Normal linewidth for this device in the single-frequency Ramsey configuration is approximately 350 Hz.

Conclusions

The two-frequency separated oscillatory field technique has the potential to remove the cavity phase-shift error which is the most serious source of error in atomic beam frequency standards. With proper beam source and state selector design, the distributed phase-shift error may likewise be eliminated. Increased stability through reduced magnetic sensitivity is also a potential benefit of this technique. However, these benefits will not be attained without a small tradeoff in terms of short-term stability.

REFERENCES

[1] N. F. Ramsey, *Molecular Beams*. London: Oxford University Press, 1956, pp. 124–144.
[2] S. Jarvis, Jr., "Molecular beam tube frequency biases due to distributed cavity phase variations," NBS Tech. Note 660, Jan. 1975.
[3] S. Jarvis, Jr., D. J. Wineland, and H. Hellwig, "Two-frequency excitation for the Ramsey separated oscillatory field method," *J. Appl. Phys.*, vol. 48, pp. 5336–5337, Dec. 1977.
[4] U. E. Kruse and N. F. Ramsey, *J. Math. Phys.*, vol. 30, p. 40, 1951.
[5] J. Picque, "Hyperfine optical pumping of a cesium atomic beam, and applications," *Metrologia*, vol. 13, pp. 115–120, 1977.
[6] D. J. Wineland, D. W. Allan, D. J. Glaze, H. W. Hellwig, and S. Jarvis, Jr., "Results on limitations in primary cesium standard operation," *IEEE Trans. Instrum. Meas.*, vol. IM-25, pp. 453–458, Dec. 1976.